Advances in Bioresearch

ORIGINAL ARTICLE

Comprehensive *In Silico* Screening of Some Indole Derivatives as Potential Selective Oestrogen Receptor Degrader (SERD)

Manjushri P. Dabhade[1,2], Pratap S. Dabhade[3]*, Gokul S. Talele[4]**
[1]SNJB's Shriman Suresh Dada Jain College of Pharmacy, Chandwad, Maharashtra, India.
[2]R. C. Patel Institute of Pharmacy, Shirpur, Maharashtra, India.
[3]*H. R. Patel Institute of Pharmaceutical Education and Research, Shirpur, Maharashtra, India.
[4]*Matoshri College of Pharmacy, Odha, Nashik Maharashtra, India.
Correspondence author email: pratap.dabhade@rediffmail.com *; gtalele@yahoo.com **

ABSTRACT
Selective estrogen receptor degraders (SERDs) have gained attention for their dual mechanism of action: they not only inhibit estrogen receptor signaling but also degrade the receptor itself, reducing ER expression levels. In this study, we conduct a comprehensive in silico screening of selected indole derivatives to evaluate their potential as selective estrogen receptor degraders. Using ADMET analysis and molecular docking techniques, we aim to identify indole derivatives with optimal pharmacokinetic properties and strong binding interactions with ERα, potentially advancing the development of novel SERDs for effective breast cancer therapy. Mostly all the compounds exhibited optimal drug-likeness properties and displayed good ADME parameters. All the designed compounds displayed either toxicity class III to V. From molecular docking, it was observed that many molecules displayed better binding free energy than native ligand and formed at least one conventional hydrogen bond with target enzyme. Native ligand displayed -8.4 kcal/mol binding affinity and did not formed any kind of conventional hydrogen bond. MDT-32, MDT-39, MDT-43, MDT-44, MDT-45, MDT-47, MDT-54, MDT-58, MDT-59, and MDT-60 had exhibited -9.4, -8.9, -9.2, -9, -9.2, -9.3, -9, -9.2, -9.1, -9 kcal/mol of binding free energies, respectively. Therefore, from present investigation, we have selected MDT-32, MDT-39, MDT-43, MDT-44, MDT-45, MDT-47, MDT-54, MDT-58, MDT-59, and MDT-60 for the wet lab synthesis and biological evaluations. From present investigation, it was concluded that, these molecules possess potential to be developed as potent SERD for the treatment of cancer.
Keywords: Indole derivatives, ADMET, Molecular docking, SERD, Cancer

INTRODUCTION
Breast cancer remains one of the most prevalent cancers worldwide, accounting for significant morbidity and mortality in women. Estrogen receptor (ER)-positive breast cancer, driven by estrogen signaling, is the most common subtype, comprising nearly 70% of all breast cancer cases. Estrogen receptors, particularly ERα, play a crucial role in tumor cell proliferation, making them a prime target for therapeutic intervention. Current treatment strategies for ER-positive breast cancers include selective estrogen receptor modulators (SERMs), aromatase inhibitors, and selective estrogen receptor degraders (SERDs). While these therapies have demonstrated efficacy, resistance to standard treatments and adverse side effects highlight the need for new SERDs with improved efficacy and safety profiles.

Selective estrogen receptor degraders (SERDs) have gained attention for their dual mechanism of action: they not only inhibit estrogen receptor signaling but also degrade the receptor itself, reducing ER expression levels. This mechanism can potentially overcome limitations of SERMs and address resistance in ER-positive cancers. However, limitations in currently available SERDs, such as poor bioavailability and off-target effects, drive the pursuit of novel compounds with optimized properties. Indole derivatives, a class of heterocyclic compounds with a wide range of biological activities, have shown promise as scaffolds for developing effective SERDs due to their structural compatibility with ER binding pockets.

In recent years, *in silico* methods have become essential in early-stage drug discovery due to their efficiency and cost-effectiveness. ADMET (Absorption, Distribution, Metabolism, Excretion, and Toxicity) analysis and molecular docking studies, as part of in silico screening, offer valuable insights into a compound's drug-likeness and binding affinity with target proteins, helping streamline the search for promising candidates. In this study, we conducted a comprehensive *in silico* screening of selected indole derivatives to evaluate their potential as selective estrogen receptor degraders. Using ADMET analysis and molecular docking techniques, we aim to identify indole derivatives with optimal pharmacokinetic properties and strong binding interactions with ERα, potentially advancing the development of novel SERDs for effective breast cancer therapy.

MATERIAL AND METHODS
Designing of Derivatives
The derivatives were designed using (E)-N-((2-(4-(1H-imidazol-1-yl)phenyl)-1H-indol-3-yl) methylene) pyridin-2-amine derivatives. The derivatives from MDT-31 to MDT-60 were designed, the different substitutions are depicted in Table 1.

Table 1. The structure of parent nucleus and different substitution used for the designing

(*E*)-*N*-((2-(4-(1*H*-imidazol-1-yl)phenyl)-1*H*-indol-3-yl)methylene)pyridin-2-amine derivatives

Derivatives Code	—R1	—R2
MDT-31	—4-COOH	—H
MDT-32	—4-fluoro	—H
MDT-33	—4-bromo	—H
MDT-34	—4-chloro	—H
MDT-35	—4-iodo	—H
MDT-36	—4-nitro	—H
MDT-37	—4-methoxy	—H
MDT-38	—4-isopropyl	—H
MDT-39	—4-trifluoromethoxy	—H
MDT-40	—4-methyl	—H
MDT-41	—4-methylthio	—H
MDT-42	—3,4-dimethoxy	—H
MDT-43	—3,4-dimethyl	—H
MDT-44	—3-methyl-4-chloro	—H
MDT-45	—2-methylthio	—H
MDT-46	—4-COOH	—OCH$_3$
MDT-47	—4-fluoro	—OCH$_3$
MDT-48	—4-bromo	—OCH$_3$
MDT-49	—4-chloro	—OCH$_3$
MDT-50	—4-iodo	—OCH$_3$
MDT-51	—4-nitro	—OCH$_3$
MDT-52	—4-methoxy	—OCH$_3$
MDT-53	—4-isopropyl	—OCH$_3$
MDT-54	—4-trifluoromethoxy	—OCH$_3$
MDT-55	—4-methyl	—OCH$_3$
MDT-56	—4-methylthio	—OCH$_3$
MDT-57	—3,4-dimethoxy	—OCH$_3$
MDT-58	—3,4-dimethyl	—OCH$_3$
MDT-59	—3-methyl-4-chloro	—OCH$_3$
MDT-60	—2-methylthio	—OCH$_3$

In silico AMDET Screening

Mol Inspiration, a free service for the online chemistry community, provides access to molecular metrics like logP, polar surface area, number of hydrogen bond donors and acceptors (GPCR ligands, kinase inhibitors, ion channel modulators, nuclear receptors), and bioactivity score prediction for the most significant drug targets. The SwissADME online tool may be used to compute physicochemical descriptors and predict ADME parameters, pharmacokinetic properties, drug-like nature, and medicinal chemistry friendliness of one or more small molecules to assist in drug development. Utilizing mol inspiration (https://www.molinspiration.com/) and SwissADME servers (http://www.swissadme.ch/), Lipinski rule of five and pharmacokinetic features of designed derivatives were investigated[1–4]. Toxicity prediction is an important phase in the development of novel medications. The use of computational toxicity estimations as opposed to animal toxic dose assessments may reduce the number of animal investigations. Toxicological endpoints, including acute toxicity, liver toxicity, cell death, carcinogenicity, mutation, immunotoxicity, unfavorable outcomes (Tox21) pathways, and toxicity targets are all covered in ProTox-arsenal II's of 33 different toxicity endpoint prediction models. This incorporates (fragment similarity-based CLUSTER cross-validation) machine learning as well as molecular similarity and fragment propensity. Utilising the freely available web server ProTox-II, an in silico assessment of the toxicity potential of designed derivatives was conducted (http://tox.charite.de/protox_II)[5].

Molecular Docking

Molecular docking is a fundamental aspect of computer-assisted drug discovery and structural molecular biology. Using a method known as "ligand-protein docking," scientists may foretell how a ligand will interact with a protein whose three-dimensional structure is already known. A precise scoring system for dockings in high-dimensional areas is essential. One may do virtual screening on a large library of compounds, grade the results, and propose structural ideas of how the ligands block the target, which is highly valuable in lead optimization[6–10]. Following an initial screening process utilizing *in silico* ADMET analysis, the selected molecules underwent subsequent molecular docking studies. In order to achieve further optimization, the derivatives underwent binding affinity studies with the target enzyme. All the selected compounds and the native ligand were docked against the Estrogen Receptor Alpha (PDB Title: A Novel Oral Selective Estrogen Receptor Down-regulator, AZD9496, drives Tumour Growth Inhibition in Estrogen Receptor positive and ESR1 Mutant Models) using Autodock vina 1.1.2 in PyRx 0.8[11]. ChemDraw Ultra 8.0 was used to draw the structures of the compounds and native ligand (mole. File format). All the ligands were subjected for energy minimization by applying Universal Force Field (UFF)[12]. The crystal structure of the enzyme with PDB ID: 5ACC was obtained from RCSB Protein Data Bank (PDB) (https://www.rcsb.org/structure/5ACC). Discovery Studio Visualizer (version-19.1.0.18287) was used to refine the enzyme structure, purify it, and get it ready for docking[13]. A three-dimensional grid box with an exhaustiveness value of 8 was created for molecular docking[11]. BIOVIA Discovery Studio Visualizer was used to locate the protein's active amino acid residues. The approach outlined by Khan et al. was used to perform the entire molecular docking procedure, identify cavity and active amino acid residues[14–20]. Figure 1 shows the revealed cavity of enzyme with the native ligand.
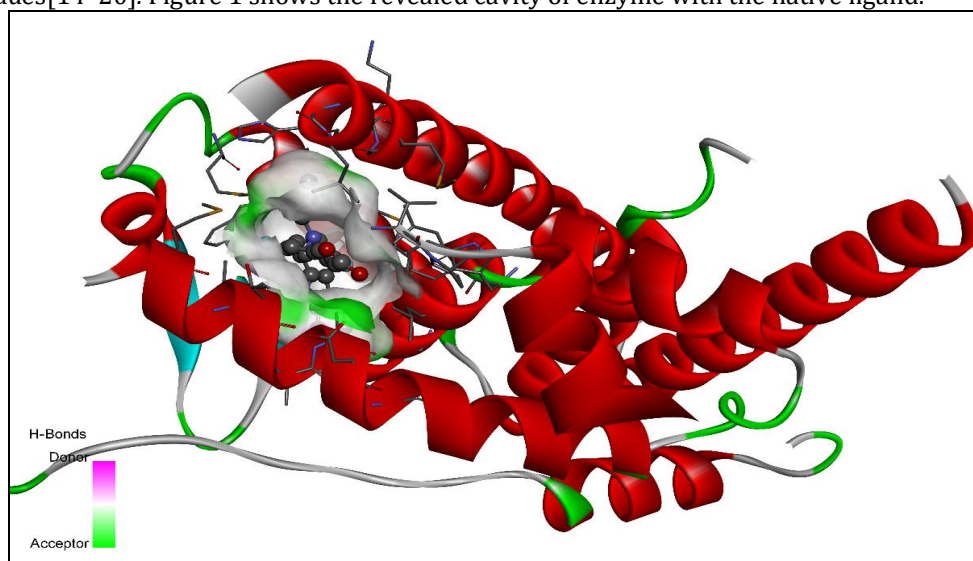

Figure 1. The 3D ribbon view of estrogen alpha receptor with native ligand (AZD9496) present in ligand binding domain

RESULTS AND DISCUSSION
In silico **ADMET Analysis**
The results of ADMET analysis are tabulated in Table 2 to 7. Lipinski's Rule of Five stands as a pivotal guideline in modern drug discovery, providing a concise set of criteria to assess the drug-likeness of small molecules based on their physicochemical properties. Introduced by Christopher A. Lipinski in 1997, this rule outlines four key parameters—molecular weight, lipophilicity, hydrogen bond donors, and hydrogen bond acceptors—to identify compounds with optimal absorption, distribution, metabolism, and excretion profiles. By adhering to these principles, researchers can efficiently filter compound libraries, reduce attrition rates, facilitate rational drug design, and integrate computational methods into the drug discovery process. Lipinski's Rule of Five serves as a cornerstone principle, guiding medicinal chemists in selecting and optimizing drug candidates with the highest probability of success, ultimately accelerating the translation of promising compounds from the laboratory to the clinic. Lipinski's Rule of Five outlines four key criteria to assess the drug-likeness of small molecules: molecular weight ≤ 500 Daltons, lipophilicity (LogP) ≤ 5, hydrogen bond donors ≤ 5, and hydrogen bond acceptors ≤ 10. These criteria serve as fundamental guidelines for evaluating a compound's potential for favorable absorption, distribution, metabolism, and excretion (ADME) profiles, crucial determinants of a drug's efficacy and safety. By adhering to these principles, researchers can efficiently screen compound libraries, prioritize molecules with optimal physicochemical properties for further development, and ultimately accelerate the drug discovery process[3,4,21]. Here in present investigation, fortunately none of the molecule displayed any major violation of Lipinski rule of five which indicates good oral bioavailability of the developed molecules.

In drug discovery, the Pfizer Rule, GSK Rule, Golden Triangle, and Chelator Rules represent critical guidelines that aid in the identification and optimization of lead compounds with desirable pharmacological properties. The Pfizer Rule and GSK Rule focus on molecular properties such as molecular weight, lipophilicity, and the number of hydrogen bond donors and acceptors, helping researchers prioritize compounds with optimal drug-like characteristics. The Golden Triangle concept emphasizes the balance between potency, selectivity, and pharmacokinetic properties, guiding the design of compounds that exhibit both therapeutic efficacy and favorable ADME profiles. Additionally, the Chelator Rules provide guidelines for the rational design of metal-binding ligands, facilitating the development of chelating agents with enhanced metal-binding affinity and selectivity for applications in imaging, diagnostics, and therapy. Together, these rules and principles serve as invaluable tools in drug discovery, guiding medicinal chemists in the efficient selection, optimization, and development of lead compounds with enhanced therapeutic potential and clinical utility[22]. It was noted that native ligand violated Pfizer rule, GSK rule, and Golden Triangle rules.

Caco-2 permeability serves as a pivotal tool in drug discovery, providing valuable insights into the intestinal absorption potential of drug candidates. Derived from human colon carcinoma cells, Caco-2 cell monolayers closely mimic the epithelial barrier of the small intestine, allowing researchers to assess a compound's ability to permeate biological membranes and predict its oral bioavailability. By measuring the permeability of compounds across Caco-2 cell monolayers, researchers can identify molecules with optimal intestinal absorption properties, guiding the selection and optimization of lead compounds early in the drug discovery process. This information is crucial for prioritizing candidates with enhanced oral bioavailability, reducing the risk of failure in later stages of development, and accelerating the translation of promising compounds from preclinical studies to clinical trials[23].

MDCK (Madin-Darby canine kidney) permeability assay holds significant importance in drug discovery as it provides crucial insights into a compound's ability to traverse biological barriers, particularly the blood-brain barrier (BBB). Derived from canine kidney cells, MDCK cells form tight epithelial monolayers similar to those found in biological barriers. By measuring a compound's permeability across MDCK cell monolayers, researchers can assess its ability to penetrate cellular membranes and predict its potential to cross the BBB. This information is vital for the development of central nervous system (CNS) drugs, as compounds must effectively penetrate the BBB to exert therapeutic effects in the brain. Thus, MDCK permeability assay plays a pivotal role in early drug screening and optimization, enabling the selection of lead candidates with enhanced CNS penetration and improved efficacy for neurological disorders[24].

In drug discovery, understanding the role of P-glycoprotein (P-gp) inhibitors and substrates is crucial for optimizing the pharmacokinetic properties of potential drug candidates. P-gp, a membrane transporter protein, plays a pivotal role in drug efflux from cells, particularly in the blood-brain barrier and gastrointestinal tract. By identifying compounds that act as P-gp inhibitors, researchers can enhance the bioavailability and efficacy of co-administered drugs by inhibiting their efflux from cells. Conversely, recognizing compounds that are substrates for P-gp enables the prediction of potential drug-drug

interactions and the design of compounds with improved pharmacokinetic profiles. Therefore, studying P-gp inhibitors and substrates is instrumental in mitigating drug resistance, improving therapeutic outcomes, and advancing the development of effective and safe medications in various therapeutic areas[25–29].

In drug discovery, the terms F20% and F30% hold significant importance as they represent the fraction of compounds that exhibit at least 20% or 30% oral bioavailability, respectively. These metrics serve as critical indicators of a compound's potential for effective absorption following oral administration. By evaluating the percentage of compounds that meet these thresholds in screening libraries or during lead optimization, researchers can gauge the overall likelihood of identifying orally bioavailable drug candidates. This information is invaluable for prioritizing compounds with favorable pharmacokinetic properties early in the drug discovery process, thereby reducing the risk of late-stage failures and expediting the development of promising therapeutics. Consequently, F20% and F30% play a pivotal role in enhancing the efficiency and success rate of drug discovery endeavors.

Table 2. Lipinski rule of 5 and Veber's rule calculated for molecules

Code	Physicochemical Property							
	Molecular Weight	Volume	nHA	nHD	nRot	TPSA	logS	logP
NL	442.19	440.779	4.0	2.0	5.0	56.33	-4.101	3.381
MDT-31	407.140	416.532	7	2	5	96.160	-4.010	4.333
MDT-32	381.140	390.359	5	1	4	58.860	-6.024	4.603
MDT-33	441.060	403.575	5	1	4	58.860	-6.478	5.215
MDT-34	397.110	399.503	5	1	4	58.860	-6.439	5.108
MDT-35	489.050	409.568	5	1	4	58.860	-6.181	5.399
MDT-36	408.130	410.232	8	1	5	102.000	-6.112	4.359
MDT-37	393.160	410.378	6	1	5	68.090	-6.021	4.539
MDT-38	405.200	436.180	5	1	5	58.860	-6.320	5.597
MDT-39	447.130	428.581	6	1	6	68.090	-6.680	5.611
MDT-40	377.160	401.588	5	1	4	58.860	-6.092	4.902
MDT-41	409.140	420.097	5	1	5	58.860	-6.230	5.130
MDT-42	423.170	436.464	7	1	6	77.320	-5.714	4.191
MDT-43	391.180	418.884	5	1	4	58.860	-6.129	5.376
MDT-44	411.130	416.799	5	1	4	58.860	-6.559	5.623
MDT-45	409.140	420.097	5	1	5	58.860	-5.989	5.047
MDT-46	437.150	442.618	8	2	6	105.390	-3.909	4.883
MDT-47	411.150	416.445	6	1	5	68.090	-6.986	5.266
MDT-48	471.070	429.661	6	1	5	68.090	-7.276	5.852
MDT-49	427.120	425.589	6	1	5	68.090	-7.238	5.756
MDT-50	519.060	435.655	6	1	5	68.090	-7.025	6.021
MDT-51	438.140	436.319	9	1	6	111.230	-7.028	4.995
MDT-52	423.170	436.464	7	1	6	77.320	-7.004	5.201
MDT-53	453.210	462.266	6	1	6	68.090	-7.062	6.210
MDT-54	477.140	454.667	7	1	7	77.320	-7.279	6.205
MDT-55	407.170	427.674	6	1	5	68.090	-6.919	5.563
MDT-56	439.150	446.183	6	1	6	68.090	-7.088	5.774
MDT-57	453.180	462.550	8	1	7	86.550	-6.675	4.829
MDT-58	421.190	444.970	6	1	5	68.090	-6.853	6.015
MDT-59	441.140	442.885	6	1	5	68.090	-7.263	6.231
MDT-60	439.150	446.183	6	1	6	68.090	-6.916	5.692

Table 3. Drug-likeness properties of designed derivatives

Code	Medicinal Chemistry						
	QED	NP score	Lipinski Rule	Pfizer Rule	GSK Rule	Golden Triangle	Chelator Rule
NL	0.504	0.054	Accepted	Rejected	Rejected	Accepted	0
MDT-31	0.407	-1.185	Accepted	Accepted	Rejected	Accepted	0
MDT-32	0.429	-1.607	Accepted	Rejected	Rejected	Accepted	0
MDT-33	0.351	-1.392	Accepted	Rejected	Rejected	Accepted	0
MDT-34	0.388	-1.121	Accepted	Rejected	Rejected	Accepted	0
MDT-35	0.258	-1.612	Accepted	Rejected	Rejected	Accepted	0

MDT-36	0.249	-1.605	Accepted	Accepted	Rejected	Accepted	0
MDT-37	0.419	-1.265	Accepted	Rejected	Rejected	Accepted	0
MDT-38	0.349	-1.245	Accepted	Rejected	Rejected	Accepted	0
MDT-39	0.333	-1.377	Accepted	Rejected	Rejected	Accepted	0
MDT-40	0.422	-1.403	Accepted	Rejected	Rejected	Accepted	0
MDT-41	0.291	-1.520	Accepted	Rejected	Rejected	Accepted	0
MDT-42	0.382	-1.085	Accepted	Accepted	Rejected	Accepted	0
MDT-43	0.395	-1.310	Accepted	Rejected	Rejected	Accepted	0
MDT-44	0.362	-1.544	Accepted	Rejected	Rejected	Accepted	0
MDT-45	0.291	-1.418	Accepted	Rejected	Rejected	Accepted	0
MDT-46	0.369	-1.178	Accepted	Accepted	Rejected	Accepted	0
MDT-47	0.398	-1.572	Accepted	Rejected	Rejected	Accepted	0
MDT-48	0.322	-1.371	Accepted	Rejected	Rejected	Accepted	0
MDT-49	0.359	-1.492	Accepted	Rejected	Rejected	Accepted	0
MDT-50	0.237	-1.577	Rejected	Rejected	Rejected	Accepted	0
MDT-51	0.226	-1.572	Accepted	Accepted	Rejected	Accepted	0
MDT-52	0.382	-1.266	Accepted	Accepted	Rejected	Accepted	0
MDT-53	0.318	-1.235	Accepted	Rejected	Rejected	Accepted	0
MDT-54	0.301	-1.361	Accepted	Accepted	Rejected	Accepted	0
MDT-55	0.392	-1.383	Accepted	Rejected	Rejected	Accepted	0
MDT-56	0.264	-1.493	Accepted	Rejected	Rejected	Accepted	0
MDT-57	0.343	-1.097	Accepted	Accepted	Rejected	Accepted	0
MDT-58	0.365	-1.296	Accepted	Rejected	Rejected	Accepted	0
MDT-59	0.333	-1.516	Accepted	Rejected	Rejected	Accepted	0
MDT-60	0.264	-1.380	Accepted	Rejected	Rejected	Accepted	0

Table 4. An absorption parameters of developed molecules

Code	Absorption						
	Caco-2 Permeability	MDCK Permeability	Pgp-inhibitor	Pgp-substrate	HIA	F20%	F30%
NL	-4.881	0.0	---	---	---	---	---
MDT-31	-5.507	1.3e-05	---	---	---	---	---
MDT-32	-4.931	3.5e-05	-	---	---	---	---
MDT-33	-4.985	2.8e-05	+++	---	---	---	---
MDT-34	-4.981	3.2e-05	--	---	---	+	---
MDT-35	-4.951	3e-05	--	---	---	+	---
MDT-36	-4.903	8e-05	---	---	---	---	---
MDT-37	-4.980	2.8e-05	++	---	---	--	---
MDT-38	-5.036	2.8e-05	+++	--	---	++	---
MDT-39	-5.071	2.5e-05	-	---	---	----	----
MDT-40	-4.999	-3.3e-05	++	--	---	++	---
MDT-41	-4.973	2.3e-05	-	--	---	-	---
MDT-42	-5.069	3e-05	+++	---	---	---	---
MDT-43	-5.113	3.6e-05	+++	---	----	---	---
MDT-44	-5.086	3.7e-05	+	---	---	--	---
MDT-45	-5.064	2.6e-05	-	--	---	+	---
MDT-46	-5.437	8.2e-06	---	---	---	---	---
MDT-47	-5.006	2.5e-05	+++	---	----	---	---
MDT-48	-5.059	2.3e-05	+++	---	---	---	---
MDT-49	-5.048	2.2e-05	+++	---	---	---	---
MDT-50	-5.021	2.2e-05	+++	---	---	---	---
MDT-51	-4.971	4.8e-05	+++	---	---	---	---
MDT-52	-5.061	1.8e-05	+++	---	---	---	---
MDT-53	-5.115	2.1e-05	+++	---	---	--	---
MDT-54	-5.148	2.2e-05	+++	---	---	---	---
MDT-55	-5.075	2.4e-05	+++	---	---	---	---
MDT-56	-5.038	1.5e-05	+++	---	---	---	---
MDT-57	-5.158	1.9e-05	+++	---	---	---	---
MDT-58	-5.190	2.3e-05	+++	---	---	---	---
MDT-59	-5.147	2.4e-05	+++	---	---	---	---
MDT-60	-5.145	1.8e-05	+++	---	---	---	---

Table 5. Distribution and metabolism profile of developed molecules

Code	Distribution				Metabolism									
	PPB (%)	VD	BBB Penetration	Fu	CYP1A2		CYP2C19		CYP2C9		CYP2D6		CYP3A4	
					Inhibitor	substrate	Inhibitor	substrate	Inhibitor	substrate	Inhibitor	substrate	Inhibitor	substrate
NL	97.9%	0.525	---	2.2	---	+++	+++	+++	+++	---	---	---	++	+++
MDT-31	97.831	0.485	--	1.311	++	--	-	---	+	--	+++	---	++	--
MDT-32	98.638	2.846	-	1.326	+++	--	++	---	++	+	+++	--	+++	-
MDT-33	98.620	2.969	--	1.290	+++	--	+++	---	+++	+	+++	--	+++	-
MDT-34	99.255	2.994	---	1.026	+++	--	+++	---	+++	+	+++	--	+++	+
MDT-35	99.156	2.237	---	1.203	+++	--	+++	---	+++	+	+++	--	+++	+
MDT-36	98.604	1.249	--	1.307	+++	--	+++	---	+++	+	+++	--	+++	-
MDT-37	98.677	2.415	--	1.167	+++	--	+++	---	+++	++	+++	-	+++	+
MDT-38	99.330	3.417	--	0.890	+++	--	+++	---	+++	+	+++	--	+++	+
MDT-39	99.69	5.833	---	0.828	+++	--	+++	---	+++	+	+++	--	+++	+
MDT-40	98.709	2.516	-	1.165	+++	--	+++	---	+++	+	+++	--	+++	+
MDT-41	98.450	2.591	-	0.921	+++	--	+++	---	+++	+	+++	--	+++	+
MDT-42	98.498	1.517	--	1.090	+++	+	+++	----	+++	++	+++	-	+++	++
MDT-43	99.149	2.509	-	1.005	+++	--	+++	---	+++	+	+++	-	+++	++
MDT-44	99.387	2.811	---	0.948	+++	--	+++	---	+++	+	+++	--	+++	+
MDT-45	98.731	2.739	-	0.886	+++	--	+++	---	+++	-	+++	--	+++	++
MDT-46	98.680	0.312	---	1.119	+++	--	+	---	++	--	+++	--	+++	--
MDT-47	99.394	2.024	--	1.251	+++	--	+++	---	+++	+	+++	-	+++	+
MDT-48	99.744	2.308	---	1.354	+++	--	+++	---	+++	+	+++	-	+++	+
MDT-49	99.600	2.195	---	1.088	+++	--	+++	---	+++	+	+++	--	+++	++
MDT-50	99.663	1.305	---	1.231	+++	--	++	---	+++	+	+++	-	+++	++
MDT-51	99.543	0.714	---	1.203	+++	--	+++	---	+++	+	+++	-	+++	+
MDT-52	99.131	1.417	---	1.163	+++	-	+++	---	+++	++	+++	+	+++	++
MDT-53	99.888	2.847	---	0.902	+++	--	+++	---	+++	++	+++	--	+++	++
MDT-54	100.134	5.495	---	1.013	+++	-	+++	---	+++	++	+++	-	+++	++
MDT-55	99.509	1.741	--	1.176	+++	--	+++	---	+++	++	+++	-	+++	++
MDT-56	99.523	1.835	---	0.920	+++	--	+++	---	+++	+	+++	--	+++	++
MDT-57	98.693	0.821	---	1.255	+++	++	+++	---	+++	++	+++	+	+++	+++
MDT-58	99.586	1.733	---	1.077	+++	-	+++	---	+++	+	+++	+	+++	++
MDT-59	99.806	2.010	---	1.030	+++	--	+++	---	+++	+	+++	-	+++	++
MDT-60	99.718	1.951	---	0.891	+++	--	+++	---	+++	-	+++	--	+++	+++

Table 6. Toxicity and excretion profile of designed molecules

Compound codes	Toxicity								Excretion	
	LD_{50} (mg/kg)	Toxicity class	Prediction accuracy (%)	Hepatotoxicity (Probability)	Carcinogenicity (Probability)	Immunotoxicity (Probability)	Mutagenicity (Probability)	Cytotoxicity (Probability)	CL	$T_{1/2}$
NL	300	3	67.38	I (0.63)	I (0.69)	A (0.98)	I (0.68)	I (0.66)	6.806	0.638
MDT-31	4000	5	54.26	A (0.61)	A (0.57)	I (0.98)	I (0.50)	I (0.68)	1.547	0.653
MDT-32	4000	5	54.26	A (0.55)	A (0.52)	I (0.68)	A (0.62)	I (0.87)	5.623	0.106
MDT-33	500	4	54.26	A (0.54)	A (0.52)	I (0.67)	A (0.61)	I (0.85)	3.137	0.135
MDT-34	200	3	54.26	I (0.5)	A (0.50)	I (0.81)	A (0.57)	I (0.87)	5.375	0.135
MDT-35	500	4	23	A (0.51)	A (0.51)	I (0.90)	A (0.61)	I (0.87)	3.736	0.096
MDT-36	500	4	54.26	A (0.59)	A (0.81)	I (0.59)	A (0.95)	I (0.78)	4.326	0.193
MDT-37	200	3	54.26	A (0.51)	A (0.58)	A (0.85)	A (0.70)	I (0.70)	6.135	0.248
MDT-38	500	4	54.26	I (0.53)	A (0.62)	I (0.73)	A (0.78)	I (0.80)	4.680	0.104
MDT-39	200	3	54.26	A (0.64)	A (0.54)	A (0.78)	A (0.54)	I (0.65)	5.788	0.150
MDT-40	100	3	54.26	A (0.51)	A (0.64)	I (0.94)	A (0.75)	I (0.90)	6.361	0.121
MDT-41	800	4	54.26	A (0.57)	A (0.59)	I (0.78)	A(0.72)	I (0.86)	5.702	0.212
MDT-42	200	3	54.26	I (0.50)	A (0.57)	A (0.67)	A (0.70)	I (0.59)	6.819	0.467
MDT-43	100	3	54.26	I (0.52)	A (0.66)	I (0.94)	A (0.79)	I (0.89)	5.698	0.139

MDT-44	200	3	54.26	I (0.50)	A (0.52)	I (0.92)	A (0.59)	I (0.88)	5.461	0.103
MDT-45	800	4	23	A (0.57)	A (0.59)	I (0.79)	A(0.72)	I (0.86)	7.067	0.124
MDT-46	4000	5	23	A (0.54)	I (0.52)	I (0.98)	A(0.60)	I (0.67)	2.249	0.483
MDT-47	4000	5	23	A (0.60)	I (0.55)	I (0.68)	A(0.58)	I (0.74)	6.539	0.057
MDT-48	1000	4	23	A (0.57)	I (0.54)	I (0.67)	A (0.58)	I (0.72)	4.217	0.064
MDT-49	1000	4	23	A (0.55)	I (0.55)	I (0.81)	A (0.58)	I (0.75)	6.297	0.069
MDT-50	1000	4	23	A (0.55)	I (0.55)	I (0.90)	A (0.59)	I (0.75)	4.905	0.051
MDT-51	1000	4	23	A (0.58)	A (0.70)	I (0.60)	A (0.91)	I (0.71)	5.775	0.097
MDT-52	200	3	54.26	I (0.51)	I (0.50)	A (0.59)	A (0.67)	I (0.73)	6.707	0.107
MDT-53	200	3	23	I (0.54)	I (0.58)	A (0.77)	A (0.64)	I (0.77)	5.603	0.054
MDT-54	200	3	23	A (0.63)	I (0.51)	A (0.74)	A (0.56)	I (0.75)	6.412	0.069
MDT-55	500	4	23	I (0.51)	A (0.50)	I (0.95)	A (0.57)	I (0.76)	6.627	0.095
MDT-56	1000	4	23	A (0.54)	A (0.52)	I (0.82)	A (0.61)	I (0.82)	7.145	0.060
MDT-57	1000	4	54.26	I (0.51)	I (0.53)	I (0.65)	A (0.66)	I (0.57)	6.991	0.219
MDT-58	500	4	23	I (0.53)	I (0.53)	I (0.95)	A (0.67)	I (0.76)	6.520	0.075
MDT-59	1000	4	23	A (0.52)	I (0.55)	I (0.93)	A (0.59)	I (0.75)	6.297	0.056
MDT-60	518	4	23	A (0.54)	A (0.52)	I (0.85)	A (0.61)	I (0.82)	7.742	0.060

Table 7. Environmental toxicity profile of designed molecules

-Code	Environmental toxicity			
	Bioconcentration Factors	IGC50	LC50FM	LC50DM
NL	1.341	3.962	5.123	5.672
MDT-31	0.211	3.255	4.804	5.062
MDT-32	2.155	4.566	5.450	5.491
MDT-33	2.533	4.886	6.095	5.437
MDT-34	2.464	4.798	5.877	5.380
MDT-35	2.769	5.051	6.155	5.431
MDT-36	1.567	4.759	5.680	5.340
MDT-37	2.091	4.621	5.663	5.411
MDT-38	2.697	4.779	5.952	5.418
MDT-39	2.133	4.614	5.863	5.509
MDT-40	2.164	4.690	5.456	5.374
MDT-41	2.106	4.565	5.474	5.333
MDT-42	2.156	4.511	5.553	5.421
MDT-43	2.399	4.758	5.583	5.369
MDT-44	2.809	4.988	6.047	5.397
MDT-45	1.857	4.679	5.697	5.295
MDT-46	0.315	3.466	5.198	5.183
MDT-47	2.633	4.744	6.109	5.743
MDT-48	3.148	5.020	6.671	5.609
MDT-49	3.077	4.944	6.548	5.501
MDT-50	3.301	5.149	6.710	5.600
MDT-51	2.056	4.904	6.309	5.486
MDT-52	2.758	4.792	6.371	5.527
MDT-53	3.184	4.927	6.601	5.537
MDT-54	2.385	4.790	6.385	5.735
MDT-55	2.780	4.737	6.111	5.477
MDT-56	2.721	4.859	6.128	5.513
MDT-57	2.739	4.692	6.283	5.587
MDT-58	3.055	4.914	6.195	5.496
MDT-59	3.353	5.100	6.660	5.539
MDT-60	2.299	4.861	6.338	5.431

Toxic doses are often given as LD_{50} values in mg/kg body weight. The LD_{50} is the median lethal dose meaning the dose at which 50% of test subjects die upon exposure to a compound. Toxicity classes are defined according to the globally harmonized system of classification of labelling of chemicals (GHS). LD_{50} values are given in [mg/kg]:

Class I: fatal if swallowed ($LD_{50} \leq 5$)

Class II: fatal if swallowed ($5 < LD_{50} \leq 50$)

Class III: toxic if swallowed ($50 < LD_{50} \leq 300$)

Class IV: harmful if swallowed ($300 < LD_{50} \leq 2000$)

Class V: may be harmful if swallowed ($2000 < LD_{50} \leq 5000$)

Class VI: non-toxic ($LD_{50} > 5000$)(5,30)

In present study, all the compounds displayed either toxicity class III to V. In drug discovery, the IGC_{50} (Inhibitory Concentration for 50% Growth) holds significant importance as a measure of a compound's potency in inhibiting the growth of cells or microorganisms. Determining the IGC_{50} value allows researchers to quantitatively assess the efficacy of a potential drug candidate in vitro, providing valuable insights into its ability to interfere with biological processes relevant to disease pathogenesis. By comparing IGC_{50} values across different compounds, researchers can prioritize molecules with superior potency for further optimization and development. Additionally, IGC_{50} data plays a crucial role in guiding structure-activity relationship (SAR) studies and rational drug design efforts, facilitating the identification of lead compounds with optimized pharmacological properties. Ultimately, the IGC_{50} serves as a key parameter in early-stage drug discovery, aiding in the selection and progression of promising candidates towards preclinical and clinical evaluation.

In drug discovery, the $LC_{50}FM$ (Lethal Concentration for 50% of the Maximum Effect) holds significant importance as a measure of a compound's toxicity or adverse effects. This metric quantifies the concentration of a compound required to produce a lethal effect in 50% of the tested population, often in animal models or cellular assays. By determining the $LC_{50}FM$, researchers can assess the safety profile of potential drug candidates and identify compounds with acceptable toxicity levels for further development. Understanding the $LC_{50}FM$ allows for the mitigation of potential safety concerns early in the drug discovery process, reducing the risk of adverse events during preclinical and clinical trials. Additionally, $LC_{50}FM$ data plays a crucial role in informing regulatory decisions and ensuring the safety of patients receiving the final drug product. Ultimately, the $LC_{50}FM$ serves as a key parameter in evaluating the overall toxicity and safety profile of potential therapeutics, guiding the selection and optimization of lead compounds for further development.

In drug discovery, the $LC_{50}DM$ (Lethal Concentration for 50% of the population under Defined Conditions) holds significant importance as a measure of a compound's toxicity or adverse effects under specific experimental conditions. This metric quantifies the concentration of a compound required to induce mortality in 50% of the tested population, typically in animal models or cellular assays. By determining the $LC_{50}DM$, researchers can assess the safety profile of potential drug candidates under defined conditions, such as exposure duration, route of administration, and environmental factors. Understanding the $LC_{50}DM$ allows for the identification of compounds with acceptable toxicity levels for further development, aiding in the selection and optimization of lead candidates while minimizing the risk of adverse events during preclinical and clinical trials. Additionally, $LC_{50}DM$ data informs regulatory decisions and contributes to the overall safety evaluation of pharmaceutical products, ensuring the well-being of patients receiving the final drug formulations[31–33].

Molecular Docking Studies

The combined docked view of all the molecules bound in ligand binding domain cavity of the receptor is given in Figure 2. The docking scores and the ligand energies (Kcal/mol) of the molecules are tabulated in Table 8. The docking interactions of most potent compounds are tabulated in Table 9. The 2D- and 3D-docking poses of the molecules are depicted in Table 10.
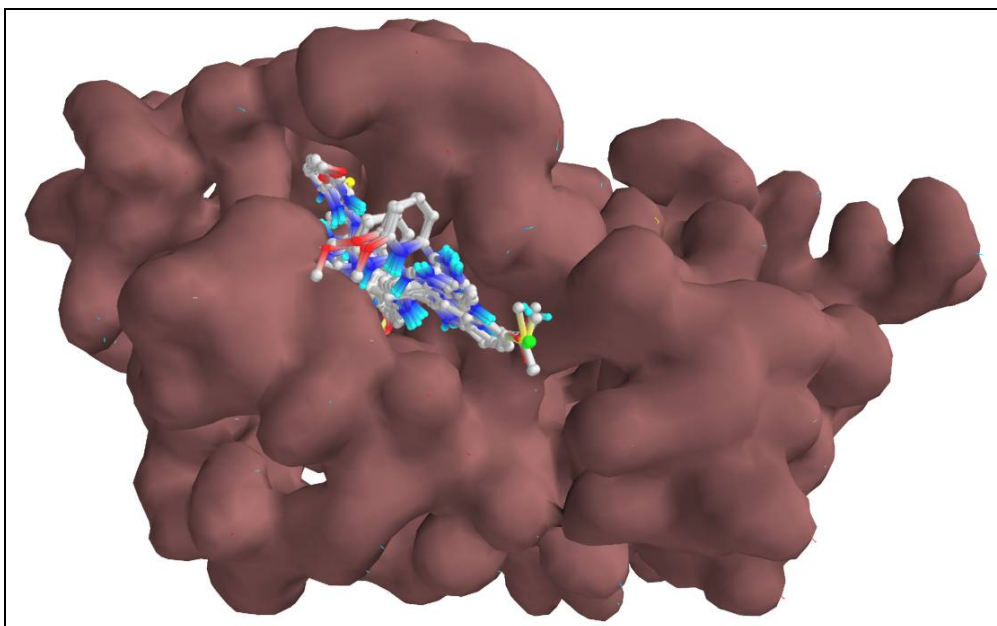
Figure 2. Binding of all the designed molecules in receptor binding domain cavity of target

Table 8. The docking scores and ligand energies (Kcal/mol) of the designed molecules in comparison with native ligand

(*E*)-*N*-((2-(4-(1*H*-imidazol-1-yl)phenyl)-1*H*-indol-3-yl)methylene)pyridin-2-amine derivatives

Ligand Code	Ligand Energy (Kcal/mol)	Binding Affinity (Kcal/mol)
MDT-31	650.56	-8.4
MDT-32	638.30	-9.4
MDT-33	637.19	-8.5
MDT-34	637.41	-8.6
-MDT-35	636.74	-8.5
MDT-36	656.16	-8
MDT-37	653.71	-8.3
MDT-38	691.61	-8.7
MDT-39	685.05	-8.9
MDT-40	637.85	-8.8
MDT-41	660.54	-8.3
MDT-42	683.13	-8.4
MDT-43	643.98	-9.2
MDT-44	642.13	-9
MDT-45	682.64	-9.2
MDT-46	662.09	-8.4
MDT-47	648.64	-9.3
MDT-48	648.71	-8.4
MDT-49	648.63	-8.7
MDT-50	647.96	-8.4
MDT-51	664.65	-8.4
MDT-52	662.82	-8.6
MDT-53	703.36	-8.6
MDT-54	697.52	-9
MDT-55	649.16	-8.7
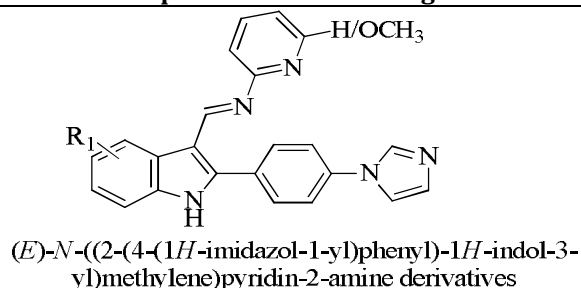
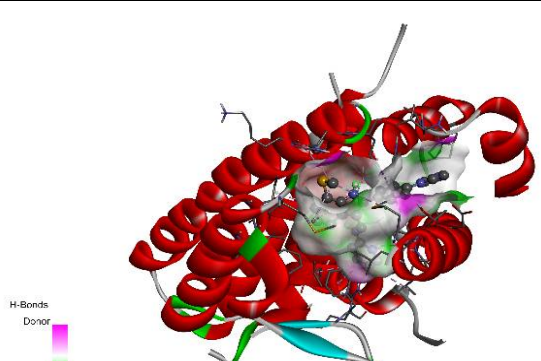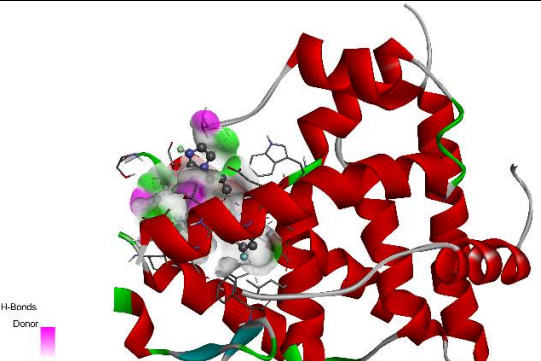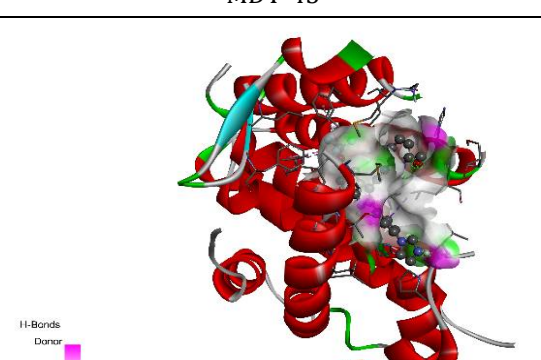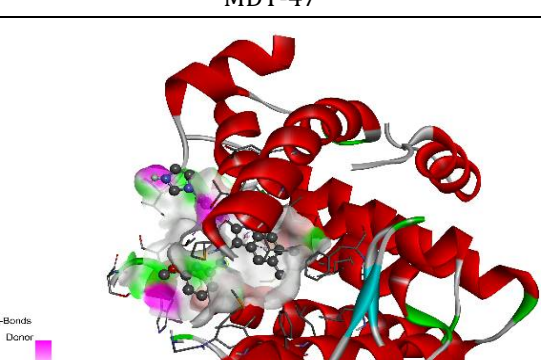|			
MDT-56	675.42	-8.3	
MDT-57	693.35	-8.4	
MDT-58	655.07	-9.2	
MDT-59	652.38	-9.1	
MDT-60	694.58	-9	
Native Ligand	413.18	-8.4	
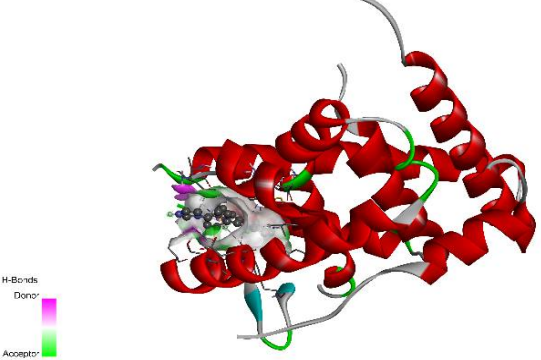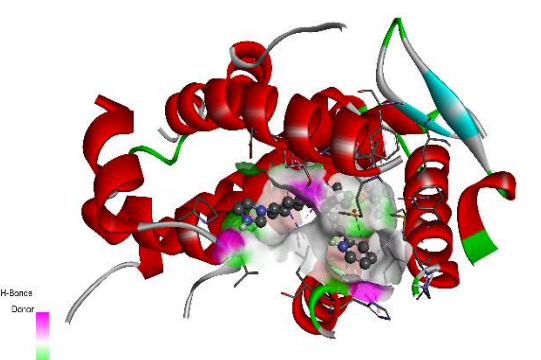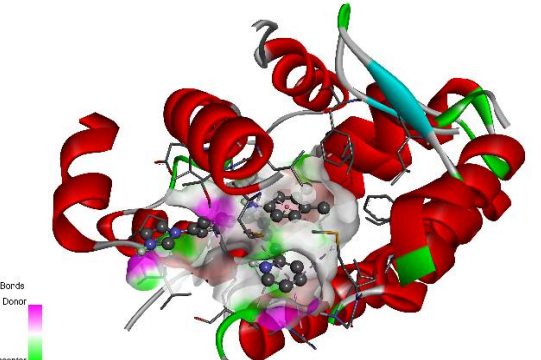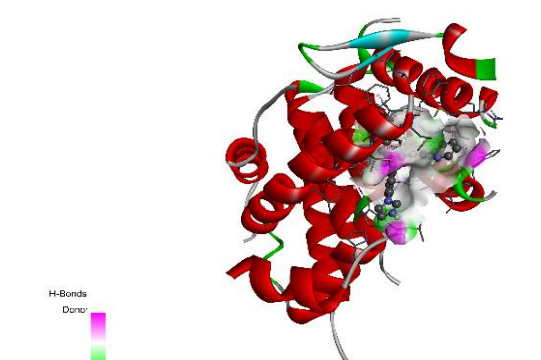
Table 9. The binding interactions of the most potent molecules which are selected for further evaluation

Active Amino Acids	Bond Length	Bond Type	Bond Category
MDT-32			
VAL533	3.62261	Hydrogen Bond	Carbon Hydrogen Bond
LEU384	3.73323		Pi-Sigma
LEU525	3.76913		
MET421	3.97303		Alkyl
ILE424	4.46971		
ALA350	4.43424	Hydrophobic	
LEU384	5.41561		
LEU387	5.04867		
LEU387	5.31934		Pi-Alkyl
MET388	4.4957		
LEU391	5.40569		
ALA350	4.22048		
HIS524	4.48205		
MDT-39			
HIS524	3.62066	Hydrogen Bond	Carbon Hydrogen Bond
LEU525	3.7787		Pi-Sigma
MET343	5.35299		Alkyl
MET421	4.11024		
LEU391	5.32884		
LEU428	5.03192		
ALA350	5.31719	Hydrophobic	
ALA350	4.29835		
LEU384	5.37005		
MET388	5.36445		Pi-Alkyl
LA350	4.71383		
PHE404	4.84013		
PHE425	4.86535		
HIS524	4.13235		
MDT-43			
VAL533	3.39598	Hydrogen Bond	Carbon Hydrogen Bond
HIS524	3.6796		
LEU525	3.70688		Pi-Sigma
MET343	5.49327		Alkyl
MET421	4.0129		
ALA350	5.20494	Hydrophobic	
ALA350	4.23643		
LEU384	5.43019		Pi-Alkyl
LEU384	5.3406		
MET388	5.34962		

ALA350	4.81034		
HIS524	4.13753		
MDT-44			
VAL533	3.42275	Hydrogen Bond	Carbon Hydrogen Bond
HIS524	3.64882		
LEU525	3.70634	Hydrophobic	Pi-Sigma
MET388	4.64571		Alkyl
LEU391	4.70557		
LEU428	4.72995		
MET343	5.44674		
MET421	4.01498		
ALA350	5.18369		Pi-Alkyl
ALA350	4.23119		
LEU384	5.41432		
LEU384	5.34341		
MET388	5.37191		
ALA350	4.8395		
PHE404	5.20861		
HIS524	4.1525		
MDT-45			
LEU346	2.69783	Hydrogen Bond	Conventional Hydrogen Bond
LEU525	3.90933	Hydrophobic	Pi-Sigma
LEU525	3.59527		
LEU349	5.13782		Alkyl
LEU391	4.34105		
MET343	5.36594		
MET421	4.01723		
MET421	4.34462		Pi-Alkyl
ILE424	4.96773		
LEU525	5.28174		
ALA350	4.35343		
PHE404	4.86286		
HIS524	4.59588		
MDT-47			
VAL533	3.57798	Hydrogen Bond	Carbon Hydrogen Bond
HIS524	3.35259		
LEU384	3.7688	Hydrophobic	Pi-Sigma
LEU525	3.73136		
MET421	3.92541		Alkyl
ILE424	4.35825		
ALA350	4.42273		Pi-Alkyl
LEU384	5.46091		
LEU387	5.03588		

LEU387	5.3373		
MET388	4.55064		
LEU391	5.38612		
ALA350	4.25477		
HIS524	4.49257		
MDT-54			
LEU525	3.79176		Pi-Sigma
LEU391	5.37483		Alkyl
LEU428	5.10248		
ALA350	5.30125	Hydrophobic	
ALA350	4.29482		
LEU384	5.49492		
LEU384	5.31321		Pi-Alkyl
MET388	5.34351		
ALA350	4.71076		
PHE404	4.84945		
PHE425	4.89467		
MDT-58			
VAL533	3.50867	Hydrogen Bond	Carbon Hydrogen Bond
LEU525	3.67361		Pi-Sigma
ALA350	4.25448		
ALA350	5.21381	Hydrophobic	
LEU384	5.33551		Pi-Alkyl
LEU384	5.43475		
MET388	5.32868		
ALA350	4.80475		
MDT-59			
VAL533	3.4564	Hydrogen Bond	Carbon Hydrogen Bond
LEU525	3.71172		Pi-Sigma
MET388	4.59883		Alkyl
LEU391	4.71006		
LEU428	4.69576		
MET343	5.49865		
MET421	4.0424		
ALA350	5.20314	Hydrophobic	
ALA350	4.24561		
LEU384	5.40341		
LEU384	5.33308		Pi-Alkyl
MET388	5.34723		
ALA350	4.80601		
PHE404	5.25038		
HIS524	4.11033		
MDT-60			
ASP351	3.43609	Hydrogen Bond	Carbon Hydrogen Bond
LEU525	3.98461		Pi-Sigma
LEU525	3.69435		
PHE404	5.72167		Pi-Pi T-shaped
MET343	4.85606		Alkyl
MET421	4.46419		
LEU387	4.78573	Hydrophobic	
LEU391	4.0562		
MET388	5.26783		
ALA350	4.26495		Pi-Alkyl
PHE404	4.89975		
HIS524	4.16211		

Table 10. The docking poses of the most potent molecules

3D-docking poses	
MDT-32	MDT-39
MDT-43	MDT-44
MDT-45	MDT-47
MDT-54	MDT-58

MDT-59

MDT-60
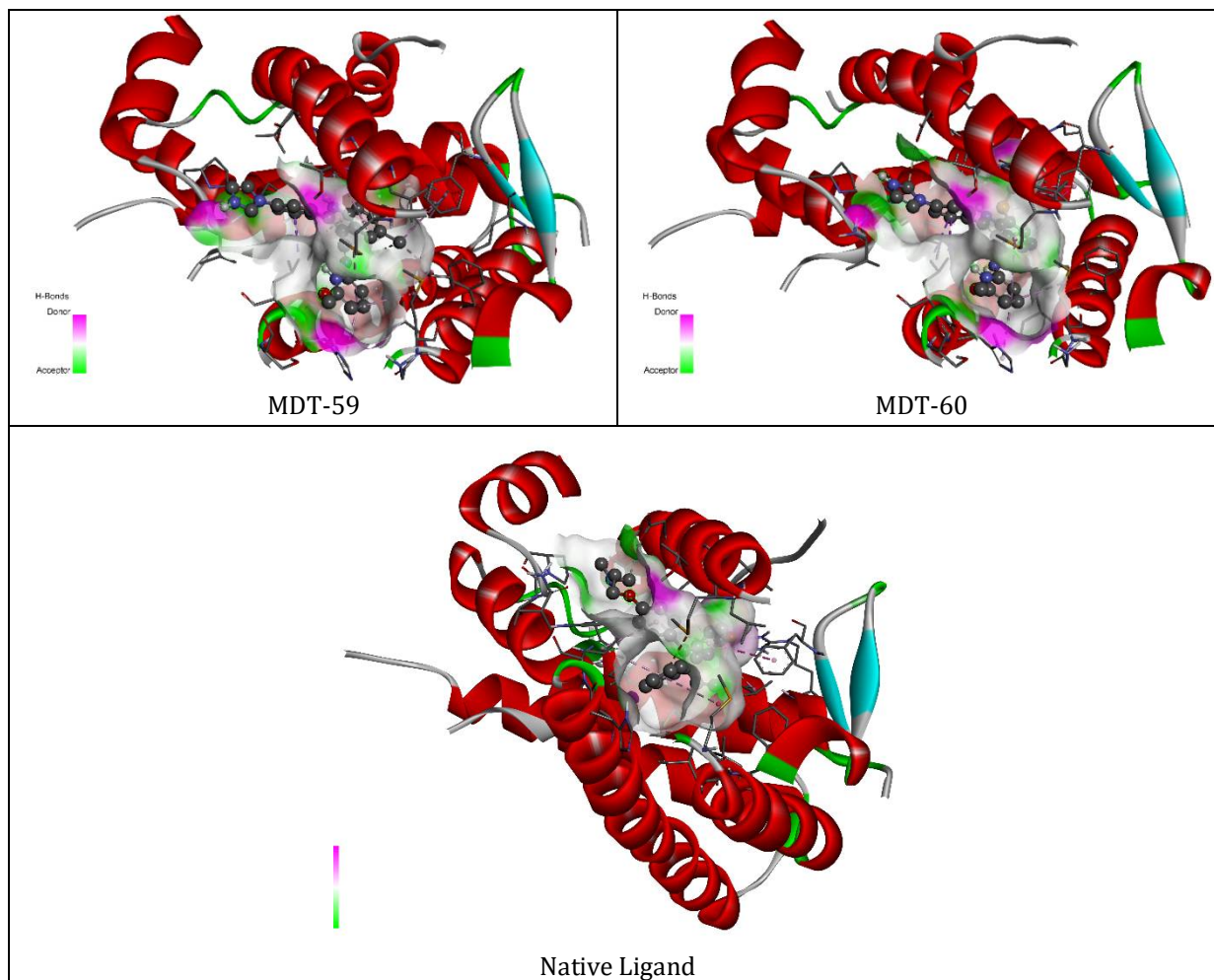
Native Ligand

From molecular docking, it was observed that many molecules displayed less binding free energy than native ligand and formed at least one hydrogen bond. Therefore, such molecules were selected for the further analysis. The discussion of those molecules are given below:

Native ligand displayed -8.4 kcal/mol binding affinity and did not formed any kind of conventional hydrogen bond. It has developed only one carbon-hydrogen bond with Asp351. It has developed few hydrophobic (Pi-sulfur, Pi-Pi T-shaped and Pi-alkyl) binds with Phe404, Ala350, Leu387, Leu391, Leu525, Met421, and Leu525. MDT-2 exhibited -9 kcal/mol binding free energy and formed one fluorinated halogen bond with Glu353. It has developed many hydrophobic interactions (Pi-sigma, alkyl, and Pi-alkyl) with Leu525, Met421, Ile424, Ala350, Leu387, Leu391, Met388, and His 524. MDT-32 exhibited -9.4 kcal/mol binding affinity with estrogen alpha and formed one carbon hydrogen bond with Val533. It has developed many hydrophobic interactions (Pi-Sigma, Alkyl, Pi-Alkyl) with Leu384, Leu525, Met421, Ile424, Ala350, Leu387, Met388, Leu391 and His524. MDT-39 displayed -8.9 kcal/mol docking score with target and developed one carbon hydrogen bond with His524. It has formed one Pi-sigma bond with Leu525. It has developed many hydrophobic (alkyl and Pi-alkyl) interactions with Met343, Met421, Leu391, Leu428, Ala350, Leu384, Met388, La350, Phe404, Phe425 and His524.

MDT-43 demonstrated -9.2 kcal/mol binding affinity and formed two carbon hydrogen bonds with Val533 and His524. It has developed numerous hydrophobic (Pi-sigma, alkyl, and Pi-alkyl) bonds with Leu525, Met343, Met421, Phe404, Leu384, Met388, Ala350 and His524. MDT-44 has formed two carbon hydrogen bonds withVal533 and His524. It exhibited -9 kcal/mol binding free energy. It has developed many hydrophobic interactions (Pi-sigma, alkyl, and Pi-alkyl) with Leu525, Met388, Leu391, Leu428, Met343, Met421, Ala350, Leu384, Phe404 and His524. MDT-45 showed -9.2 kcal/mol binding energy with target and formed one conventional hydrogen bond with Leu525. It has developed many hydrophobic interactions with Leu525, Met343, Leu391, Met421, Ala350, Met421, Phe404 and His524. MDT-47 has formed two carbon hydrogen bonds with Val533 and His524. It has formed several

hydrophobic interactions (Pi-sigma, alkyl, and Pi-alkyl) with Leu525, Met388, Leu391, Met421, Ile424, Ala350, and His524. It displayed -9.3 kcal/mol binding affinity with estrogen alpha receptor.

MDT-54 showed -9 kcal/mol binding affinity with target and it has developed many hydrophobic interactions with Leu525, Met388, Leu391, Leu428, Ala350, Leu384, Phe404 and Phe425. MDT-58 displayed -9.2 kcal/mol binding free energy and developed one carbon hydrogen bond with Val533. It has developed many hydrophobic interactions with Leu525, Met388, Leu384 and Ala350. MDT-59 displayed -9.1 kcal/mol binding free energy and developed one carbon hydrogen bond with Val533. It has developed many hydrophobic interactions with leu525, Met388, Leu391, Leu391, Leu428, Met343, Met421, Ala350, Leu384, Phe404 and His524.MDT-60 exhibited -9 kcal/mol binding affinity with estrogen alpha and formed one carbon hydrogen bond with Asp351. It has developed many hydrophobic interactions with Leu525, Phe404, Met343, Met421, Leu387, Leu391, Met388, Ala350, and His524.

As these molecules formed more stable complex with target receptor, therefore from present investigation, we have selected MDT-32, MDT-39, MDT-43, MDT-44, MDT-45, MDT-47, MDT-54, MDT-58, MDT-59, and MDT-60 for the wet lab synthesis and biological evaluations.

CONCLUSION

This study aimed to explore the potential of indole derivatives as SERDs by conducting an in-depth in silico screening using ADMET analysis and molecular docking. The objective was to identify compounds with favorable pharmacokinetic profiles and strong binding affinities for ERα, which could serve as effective SERDs for breast cancer therapy. The results showed that most indole derivatives demonstrated optimal drug-likeness with favorable ADME parameters. Toxicity analysis indicated that the compounds fell within toxicity classes III to V, signifying manageable safety profiles. Molecular docking studies further revealed that several compounds, including MDT-32, MDT-39, MDT-43, MDT-44, MDT-45, MDT-47, MDT-54, MDT-58, MDT-59, and MDT-60, exhibited higher binding free energies than the native ligand, with values ranging from -8.4 to -9.4 kcal/mol. Notably, these compounds also formed one or more conventional hydrogen bonds with the target enzyme, unlike the native ligand, which showed a binding affinity of -8.4 kcal/mol but did not form hydrogen bonds. In conclusion, the findings indicate that selected indole derivatives exhibit promising attributes as SERD candidates for breast cancer treatment. Compounds MDT-32, MDT-39, MDT-43, MDT-44, MDT-45, MDT-47, MDT-54, MDT-58, MDT-59, and MDT-60 are strong candidates for further exploration through wet lab synthesis and biological evaluation. These molecules hold significant potential to be developed into potent and selective SERDs, offering a novel approach to cancer therapy by effectively targeting estrogen receptor degradation.

REFERENCES

1. Oprea TI (2002). Virtual screening in lead discovery: A viewpoint. Molecules.;7(1):51–62.
2. Quinn RJ, Carroll AR, Pham NB, Baron P, Palframan ME, Suraweera L, et al. (2008) Developing a drug-like natural product library. J Nat Prod. 71(3):464–8.
3. Barret R. (2018) Lipinski's Rule of Five. In: Therapeutical Chemistry. p. 97–100.
4. Lipinski CA. (2016) Rule of five in 2015 and beyond: Target and ligand structural limitations, ligand chemistry structure and drug discovery project decisions. Vol. 101, Advanced Drug Delivery Reviews. p. 34–41.
5. Banerjee P, Eckert AO, Schrey AK, Preissner R. (2018) ProTox-II: A webserver for the prediction of toxicity of chemicals. Nucleic Acids Res. 46(W1):W257–63.
6. Panneerselvam S, Yesudhas D, Durai P, Anwar MA, Gosu V, Choi S. (2015) A combined molecular docking/dynamics approach to probe the binding mode of cancer drugs with cytochrome P450 3A4. Molecules.20(8):14915–35.
7. Pagadala NS, Syed K, Tuszynski J. (2017)Software for molecular docking: a review. Biophys Rev. 9(2):91–102.
8. Diller DJ, Merz KM. (2001) High throughput docking for library design and library prioritization. Proteins Struct Funct Genet.;43(2):113–24.
9. Morris GM, Lim-Wilby M. (2008) Molecular docking. Methods Mol Biol. 443:365–82.
10. Dar AM, Mir S. (2017) Molecular Docking: Approaches, Types, Applications and Basic Challenges. J Anal Bioanal Tech. 08(02).
11. Dallakyan S, Olson AJ. (2015) Small-molecule library screening by docking with PyRx. Methods Mol Biol. 1263(1263):243–50.
12. Rappé AK, Casewit CJ, Colwell KS, Goddard WA, Skiff WM. (1992) UFF, a Full Periodic Table Force Field for Molecular Mechanics and Molecular Dynamics Simulations. J Am Chem Soc. 114(25):10024–35.
13. San Diego (2012): Accelrys Software Inc. Discovery Studio Modeling Environment, Release 3.5. Accelrys Softw Inc.
14. Khan SL, Siddiqui FA, Jain SP, Sonwane GM. (2020) Discovery of Potential Inhibitors of SARS-CoV-2 (COVID-19) Main Protease (Mpro) from Nigella Sativa (Black Seed) by Molecular Docking Study. Coronaviruses. 2(3):384–402.
15. Chaudhari RN, Khan SL, Chaudhary RS, Jain SP, Siddiqui FA. (2020) B-Sitosterol: Isolation from Muntingia

Calabura Linn Bark Extract, Structural Elucidation And Molecular Docking Studies As Potential Inhibitor of SARS-CoV-2 Mpro (COVID-19). Asian J Pharm Clin Res. 13(5):204–9.

16. Khan SL, Siddiqui FA, Shaikh MS, Nema N V., Shaikh AA. (2021) Discovery of potential inhibitors of the receptor-binding domain (RBD) of pandemic disease-causing SARS-CoV-2 Spike Glycoprotein from Triphala through molecular docking. Curr Chinese Chem. 01.

17. Khan SL, Sonwane GM, Siddiqui FA, Jain SP, Kale MA, Borkar VS. (2020) Discovery of Naturally Occurring Flavonoids as Human Cytochrome P450 (CYP3A4) Inhibitors with the Aid of Computational Chemistry. Indo Glob J Pharm Sci. 10(04):58–69.

18. Siddiqui FA, Khan SL, Marathe RP, Nema N V. (2021) Design, Synthesis, and In Silico Studies of Novel N-(2-Aminophenyl)-2,3- Diphenylquinoxaline-6-Sulfonamide Derivatives Targeting Receptor- Binding Domain (RBD) of SARS-CoV-2 Spike Glycoprotein and their Evaluation as Antimicrobial and Antimalarial Agents. Lett Drug Des Discov. 18(9):915–31.

19. 19. Shntaif AH, Khan S, Tapadiya G, Chettupalli A, Saboo S, Shaikh MS, et al. (2021) Rational drug design, synthesis, and biological evaluation of novel N-(2-arylaminophenyl)-2,3-diphenylquinoxaline-6-sulfonamides as potential antimalarial, antifungal, and antibacterial agents. Digit Chinese Med. 4(4):290–304.

20. Khan S, Kale M, Siddiqui F, Nema N. (2021) Novel pyrimidine-benzimidazole hybrids with antibacterial and antifungal properties and potential inhibition of SARS-CoV-2 main protease and spike glycoprotein. Digit Chinese Med. 4(2):102–19.

21. Owens J, Lipinski CA. (2003) Chris Lipinski discusses life and chemistry after the Rule of Five. Drug Discov Today; 8(1):12–6.

22. Johnson TW, Dress KR, Edwards M. (2009) Using the Golden Triangle to optimize clearance and oral absorption. Bioorganic Med Chem Lett. 19(19):5560–4.

23. Caron J, Domenger D, Dhulster P, Ravallec R, Cudennec B. (2017) Using Caco-2 cells as novel identification tool for food-derived DPP-IV inhibitors. Food Res Int. 92:113–8.

24. Feng B, West M, Patel NC, Wager T, Hou X, Johnson J, et al. (2019) Validation of Human MDR1-MDCK and BCRP-MDCK Cell Lines to Improve the Prediction of Brain Penetration. J Pharm Sci. 108(7):2476–83.

25. Perrière N, Yousif S, Cazaubon S, Chaverot N, Bourasset F, Cisternino S, et al. (2007) A functional in vitro model of rat blood-brain barrier for molecular analysis of efflux transporters. Brain Res. 1150(1):1–13.

26. Dallavalle S, Dobričić V, Lazzarato L, Gazzano E, Machuqueiro M, Pajeva I, et al. (2020) Improvement of conventional anti-cancer drugs as new tools against multidrug resistant tumors. Drug Resist Updat. 50.

27. Fantoukh OI, Dale OR, Parveen A, Hawwal MF, Ali Z, Manda VK, et al. (2019) Safety Assessment of Phytochemicals Derived from the Globalized South African Rooibos Tea (Aspalathus linearis) through Interaction with CYP, PXR, and P-gp. J Agric Food Chem. 67(17):4967–75.

28. Raghava KM, Lakshmi PK. (2012) Overview of P-glycoprotein inhibitors: A rational outlook. Brazilian J Pharm Sci. 48(3):353–67.

29. Urgaonkar S, Nosol K, Said AM, Nasief NN, Bu Y, Locher KP, et al. (2022) Discovery and Characterization of Potent Dual P-Glycoprotein and CYP3A4 Inhibitors: Design, Synthesis, Cryo-EM Analysis, and Biological Evaluations. J Med Chem.;65(1):191–216.

30. Drwal MN, Banerjee P, Dunkel M, Wettig MR, Preissner R (2014). ProTox: A web server for the in silico prediction of rodent oral toxicity. Nucleic Acids Res.;42(W1). doi: 10.1093/nar/gku401.

31. van de Waterbeemd H, Gifford E. (2003) ADMET in silico modelling: Towards prediction paradise? Nat Rev Drug Discov. 2(3):192–204.

32. Vawhal PK, Jadhav SB, Kaushik S, Panigrahi KC, Nayak C, Urmee H, et al. (2023) Coumarin-Based Sulfonamide Derivatives as Potential DPP-IV Inhibitors: Pre-ADME Analysis, Toxicity Profile, Computational Analysis, and In Vitro Enzyme Assay. Molecules. 28(3). https://doi.org/10.3390/molecules28031004

33. Gandla K, Islam F, Zehravi M, Karunakaran A, Sharma I, Haque MA, et al. (2023) Natural polymers as potential P-glycoprotein inhibitors: Pre-ADMET profile and computational analysis as a proof of concept to fight multidrug resistance in cancer. Heliyon. 9(9). doi: 10.1016/j.heliyon.2023.e19454